JTTEE5 14:480-486
DOI: 10.1361/105996305X76487
1059-9630/$19.00 © ASM International

Peer Reviewed

Phase Formation of Nano-TiO_2 Particles during Flame Spraying with Liquid Feedstock

Guan-Jun Yang, Chang-Jiu Li, and Yu-Yue Wang

(Submitted September 20, 2004; in revised form November 19, 2004)

The nanostructured TiO_2 photocatalytic coatings were synthesized through flame spraying with liquid feedstock under different conditions. The nanostructured TiO_2 deposit of substantial anatase phase was annealed at different temperatures. X-ray diffraction analysis showed that significant transformation from anatase to rutile occurred at a temperature above 600 °C. However, thermal analysis suggested that the phase transformation from anatase to rutile started at a temperature from 400 to 500 °C. It was found that the grain size of rutile phase was larger than that of anatase. The deposits annealed at temperatures lower than 450 °C were photocatalytically active. However, the deposit annealed at 500 °C, which contained 95% anatase crystalline, became photocatalytically inactive. Based on the experimental findings, a model is proposed to explain the phase transformation of the nano-TiO_2 particles and the phase formation in flame-spraying of nanostructured TiO_2 deposit with liquid feedstock.

Keywords flame spraying with liquid feedstock, nanoparticle, phase formation, phase transformation, photocatalytic coating, TiO_2

1. Introduction

Titanium dioxide (TiO_2) is widely used in photocatalytical, optical, electrical, and tribological applications (Ref 1-5). The performance of TiO_2 is significantly influenced by the crystalline structure. For example, TiO_2 as a photocatalyst in anatase phase presents a higher photocatalytic activity than that in rutile phase (Ref 6-8). Three types of crystalline structures, including anatase, rutile, and brookite are usually present in the synthesized TiO_2, synthesized through sol-gel, vapor deposition, thermal spraying, etc. (Ref 1-5). Among three phases, rutile is a thermally stable phase. Anatase and brookite crystalline will transform to rutile as they are annealed at temperatures from 450 to 1100 °C (Ref 9-13). Therefore, the controlling of the crystalline structure of TiO_2 coating through processing is of essential importance to control the property and performance of TiO_2 deposits.

Thermal spraying with liquid feedstock was reported to fabricate nanostructured ceramics such as ZrO_2 and Al_2O_3 (Ref 14-16). The author's previous study revealed that the nanostructured TiO_2 deposits can be synthesized through flame spraying with a solution of butyl titanate as liquid feedstock (Ref 17-18). During spraying, butyl titanate is decomposed to form TiO_2, which is deposited onto a substrate in the form of nano-sized particles. The deposit is constituted mainly of anatase TiO_2 with a small fraction of rutile TiO_2. The crystalline structure of the TiO_2 deposit was influenced by spraying conditions including the atomizing conditions of the feedstock, the concentration of butyl titanate in the solution, and processing parameters. However, the grain size of rutile estimated by the Scherrer formula was larger than that of anatase.

The aim of this paper is to clarify the phase formation during the flame spraying of TiO_2 coating with liquid feedstock through the examination of the phase evolution in spraying and post-annealing.

2. Materials and Experimental Procedures

2.1 Materials

Butyl titanate [$Ti(OC_4H_9)_4$] (Xingta, Shanghai, People's Republic of China) was used as the liquid precursor to form the TiO_2 deposit. Butyl titanate was diluted in an analytically pure ethanol (Ante, Suzhou, People's Republic of China) to make the solution with a concentration of 30% for spraying. A stainless steel plate sample with dimensions of 105 × 25 × 1.5 mm was used as a substrate for the coating deposition. Prior to spraying, the substrate was blasted with 24 mesh alumina grit.

2.2 Deposition of the Coating

A liquid flame spraying torch was used to fabricate TiO_2 coatings, and the details of the torch design can be found elsewhere (Ref 17). Typical spraying conditions are shown in Table 1. Propane was used as fuel gas. Flame power resulting from the combustion of fuel gas was calculated according to combustion heat of propane. Oxygen was used as the atomizing gas. During the coating deposition, the spray torch was manipulated by a robot (Motoman, Kitakyushu) and traversed at a speed of 500 mm/s relative to the substrate. The temperature of the substrate was measured by an infrared (IR) thermodetector (RAYRPM30L3U, Santa Cruz, CA). The spraying was repeated for several passes; meanwhile, the temperature of the substrate during deposition was lower than 200 °C.

The original version of this paper was published as part of the DVS Proceedings: "Thermal Spray Solutions: Advances in Technology and Application," International Thermal Spray Conference, Osaka, Japan, 10-12 May 2004, CD-Rom, DVS-Verlag GmbH, Düsseldorf, Germany.

Guan-Jun Yang, Chang-Jiu Li, and **Yu-Yue Wang,** State Key Laboratory for Mechanical Behavior of Materials, School of Materials Science and Engineering, Xi'an Jiaotong University, Xi'an, Shaanxi, 710049 People's Republic of China. Contact e-mail: licj@mail.xjtu.edu.cn.

Table 1 Typical flame spraying parameters

Parameter		Value
Propane	Pressure	0.1 MPa
	Flow	7.3 l/min
Oxygen	Pressure	0.5 MPa
	Flow	43 l/min
Atomizing gas	Pressure	0.3 MPa
	Flow	70 l/min
Spray distance		150 mm
Feed rate of liquid feedstock		10 ml/min

2.3 Characterization of the Coating

An x-ray diffraction (XRD) system (Rigaku D/max-2400, Tokyo, Japan) was used to determine the phase constitution and grain size of the deposit. XRD analysis was carried out using Cu K_α radiation at 40 kV and 100 mA with a scan speed of 2 °/min for 2θ. Peak area was used as peak intensity to estimate the anatase content in the nanostructured coating:

$$C_A = \frac{A_A}{A_A + 1.265 \cdot A_R} \cdot 100\% \quad \text{(Eq 1)}$$

where C_A is the anatase content in the deposit, and A_R and A_A are the areas covered by rutile peak (110) and anatase peak (101) in the XRD pattern, respectively. The grain size was estimated by the Scherrer formula. The morphology of the nano-sized particles in the coating was examined through transmission electron microscopy (TEM; JEM-200CX, Tokyo, Japan). Thermal analyses including thermal gravimetry (TG) and differential thermal analysis (DTA) were carried out using thermal analyzer (TGA51, TA2000, New Castle, DE) at a heating speed of 20 °C/min.

The phase transformation from anatase to rutile in the nanostructured TiO_2 was also examined through investigation of the photocatalytic performance of TiO_2 coatings to degrade acetaldehyde under ultraviolet (UV) irradiation with a dominant wavelength at 360 nm. A quartz cuvette with the dimensions of Φ26 × 220 mm was used as the photocatalytic reactor. The radiant intensity at the coating surface was about 30 W/m^2. The acetaldehyde concentration in the cuvette was determined by gas chromatography (GC; Agilent 6890, Little Falls, CA). The photocatalytic activity was estimated by fitting the change of the relative concentration of acetaldehyde with irradiation time with the following Langmuir-Hinshelwood equation:

$$\ln(c) = -\frac{t}{\tau} \quad \text{(Eq 2)}$$

where c is the relative concentration of acetaldehyde, t is the irradiation time, and τ is the time constant of photocatalytic degradation. According to Eq 2, the smaller the value of τ, the better the photocatalytic performance of the coating. In the current study, the photocatalytic activity of the TiO_2 coating was defined as the reciprocal of τ.

3. Results

3.1 Effect of Spray Parameters on Phase Formation

Figure 1 shows the cross-sectional morphology of the coating sprayed on a glass substrate for 10 passes under typical spray conditions in Table 1. The coating thickness was estimated to be around 30 μm according to the photograph. It proved that the TiO_2 coating was formed on the substrate surface. TEM investigation revealed that the primary particles in the coating presented nano-size, and the average particle diameter was estimated to be 14 nm (Ref 17). Figure 2 shows the influence of spray distance on the anatase content in the as-sprayed coating. In comparison with 58% anatase content in the coating sprayed at a distance of 100 mm, the anatase content in the coating deposited at a spray distance of 150 mm increased to 95%. As the distance was increased from 150 to 250 mm, the anatase content of 95% was present in all coatings. Figure 3 illustrates the effects of flame power on the anatase content and the grain size in the coatings sprayed at 150 mm. As the flame power increased from 12 to 17 kW at a spray distance of 150 mm, the anatase content decreased from 95 to 29%. With further increase of the flame power to 21.8 kW, the anatase content decreased to 22%. It can be seen (Fig. 3b) that the grain sizes of rutile and anatase phases were increased with the increase of the flame power. Moreover, it can be clearly recognized that the grain size of rutile was larger than that of anatase regardless of the anatase content in the coatings.

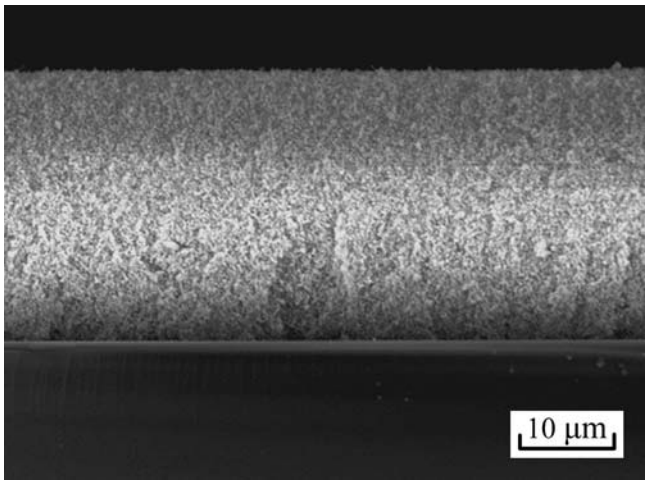

Fig. 1 Cross-sectional morphology of the coating sprayed for 10 passes

3.2 Effect of Annealing Treatment on the Microstructure of the TiO_2 Deposit

Figure 4 shows the XRD patterns of the as-sprayed TiO_2 coating and the TiO_2 coatings after annealing treatment. Figure 5 shows the effect of the annealing temperature on the crystalline structure of the coating annealed at different temperatures for 30 min. The coating was deposited under conditions shown in Table 1. From XRD patterns of these coatings, it was found that no significant phase change occurred to the coatings annealed at temperatures below 600 °C. Moreover, the anatase content was decreased with the increase of the annealing temperature from 600 °C. It was found that the grain size of rutile was always larger than that of anatase for the coatings annealed at temperatures above 650 °C. Figure 6 shows the morphologies of nano-sized particles within the as-sprayed coating and the annealed coatings at different temperatures of 650, 750, and 800 °C. The

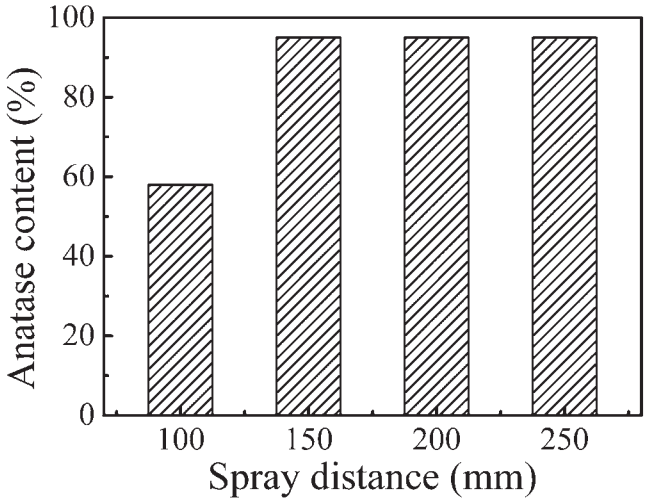

Fig. 2 Effect of spray distance on anatase content in the as-sprayed TiO_2 coating

TEM examination of the coating confirmed that no significant change in the size of the primary nanoparticles within the coatings occurred under the annealing conditions in the current study.

Figure 7 shows experimental results obtained through TG and DTA for the as-sprayed TiO_2 deposit detached from the substrate. It can be recognized that the weight loss took place within three temperature ranges. Temperature rising from room temperature to 200 °C resulted in about 4% weight loss. The next temperature change from 200 to 400 °C led to 2% weight loss, and the further heating from 600 to 800 °C yielded 1.3% weight loss. The DTA curve in Fig. 5 shows a very wide endothermic peak nearly covering the whole temperature range in the experiment.

3.3 Effect of Annealing Treatment on Photocatalytic Performance of the TiO_2 Coating

Figure 8 shows the change of the relative concentration of acetaldehyde with irradiation time using typical TiO_2 coatings compared with the result obtained without coating. The coating was deposited under conditions shown in Table 1. Without coating, 20% acetaldehyde was decomposed in 40 min by the photolysis of acetaldehyde under 360 nm ultraviolet irradiation. It is clearly seen that 90% acetaldehyde was photocatalytically degraded with the as-sprayed coating and the coating annealed at 450 °C. Moreover, the coating annealed at 500 °C did not present photocatalytic activity to degrade acetaldehyde when compared with the result only by the ultraviolet irradiation.

Figure 9 represents the effect of the annealing temperature on the photocatalytic activity of the annealed TiO_2 coatings. The as-sprayed coatings in anatase phase presented much higher photocatalytic activity than that in rutile phase annealed at 800 °C. The photocatalytic activity of the coatings annealed at temperatures from room temperature to 450 °C was the same as that of the as-sprayed one. However, the activity was significantly decreased when the coating was annealed at temperatures higher than 450 °C.

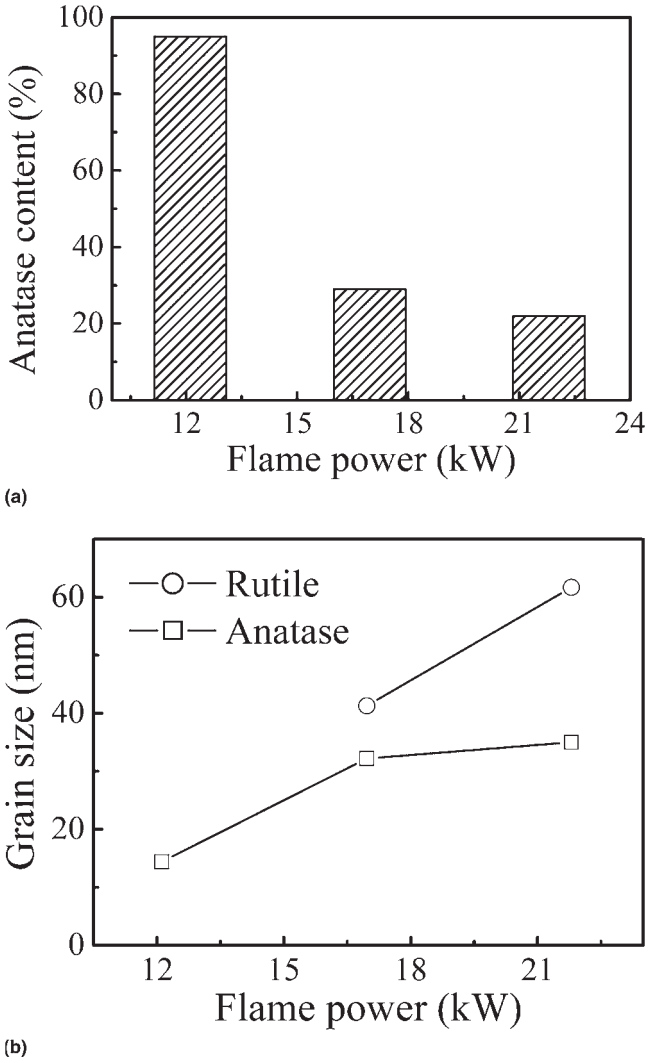

Fig. 3 Effects of flame power on (a) anatase content and (b) grain sizes of both anatase phase and rutile phase in the as-sprayed TiO_2 coating

4. Discussion

Thermal analysis yielded a total 7.3% weight loss for the as-sprayed coating when it was heated from room temperature to 800 °C. It can be considered that 4% weight loss from room temperature to 200 °C resulted from the release of physisorbed water on the TiO_2 particles surface. The 3.3% weight loss in total from 200 to 800 °C can be attributed to the desorption of the hydroxyl (OH) group on the TiO_2 surface (Ref 19, 20). The decalescence below 400 °C is caused by the desorption of water and OH group, which needs energy to leave the surface of TiO_2 particles. The differential temperature decreased continuously by 2 °C with the increase of the temperature till 400 °C, which corresponds to 6% weight loss due to the desorption of water and OH group from the TiO_2 surface. With the further heating from 400 to 1000 °C, the differential temperature turned to increase with the increase of the temperature. Because there was no obvious particle coarsening within the coating, it can be considered that the temperature increasing resulted from the phase trans-

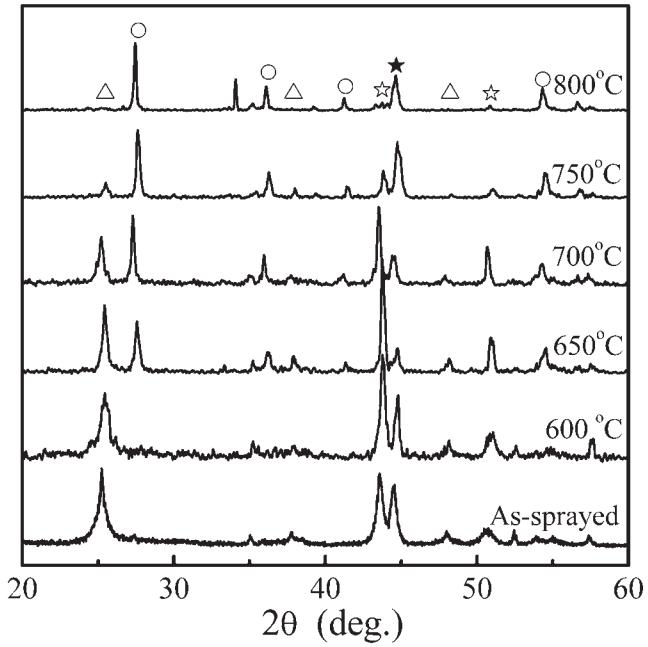

Fig. 4 XRD patterns of the as-sprayed TiO_2 coating and the TiO_2 coatings after annealing treatment: (△) anatase, (○) rutile, (☆) γ-Fe, (★) α-Fe

formation from anatase to rutile, although XRD analysis did not detect the onset of the phase transformation until 600 °C. As a result, it can be considered that the phase transformation from anatase to rutile started at around 450 °C.

Moreover, the deposits annealed at temperatures lower than 450 °C presented photocatalytic activity similar to that of the as-sprayed one. However, the deposit annealed at a temperature of 500 °C that contained about 95% anatase became photocatalytically inactive. Despite the anatase content change from 95 to 0% in the deposits annealed at temperatures higher than 500 °C, those deposits presented no significant difference in the photocatalytic activity. Because no obvious particle coarsening was observed in the deposits after annealing treatment under the present conditions, the surface areas of the deposits annealed at different temperatures should have no significant change. Therefore, taking thermal analysis into account, it can be considered that the difference in the photocatalytic activity was attributed to the phase transformation from anatase to rutile.

XRD analysis revealed that the grain size of rutile was larger than that of anatase. Taking the results of thermal analysis and the photocatalytic activity into account, it can be considered that the phase transformation from anatase to rutile started at the surface of the nano-sized particles, as schematically shown in Fig. 10. When the nanostructured TiO_2 coating is annealed at temperatures higher than 450 °C, the nucleation of rutile crystalline takes place at certain sites of the particle surface. The preferable growth of the rutile phase near the particle surface layer may form a shell of rutile covering on the anatase core. Once a complete rutile shell is formed, the surface of the particles shows little photocatalytic activity due to the much limited photocatalytic activity of the rutile phase compared with the anatase phase. Consequently, the coatings annealed at temperatures

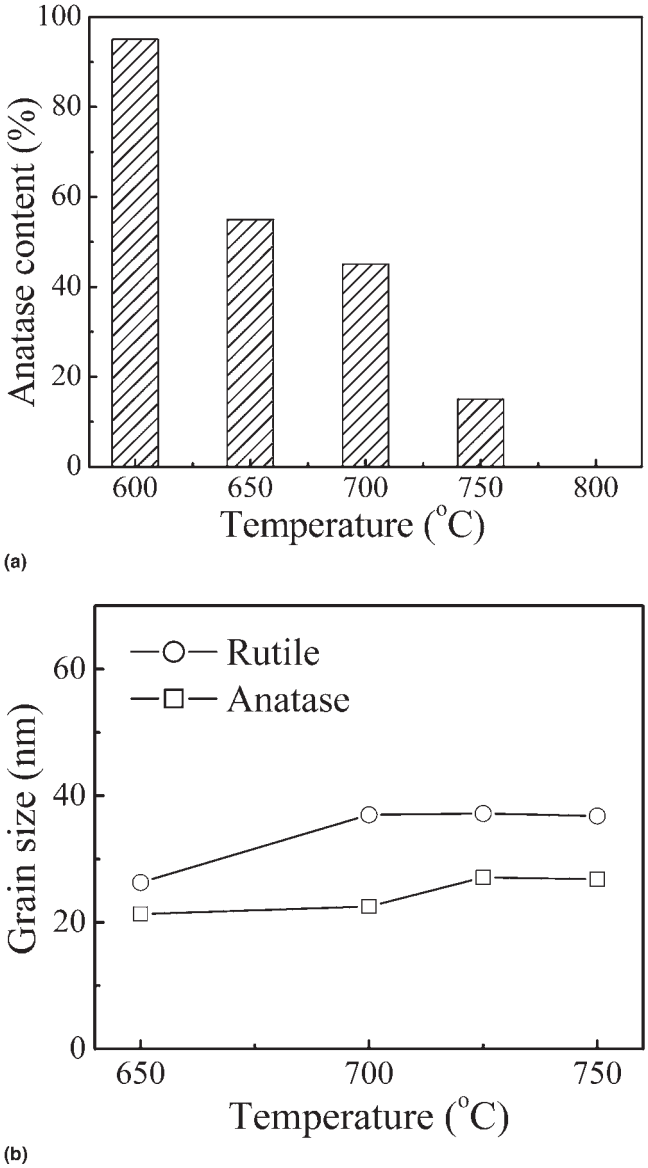

Fig. 5 Effects of annealing temperature on (a) anatase content and (b) grain size within the TiO_2 coating

higher than 450 °C presents the similar photocatalytic inactivity regardless of their much different anatase content.

During spraying, the butyl titanate is decomposed to form TiO_2 through heating of the flame. The formation of the anatase phase within the coatings sprayed at distances of 150-250 mm means that nearly pure anatase is synthesized and should be deposited in the form of nanostructured TiO_2 coating on the substrate because the phase transformation from rutile to anatase is irreversible. The result showed that when the spray distance was kept at 100 mm, about 42% rutile was present in the coating. It was found that with the parameters shown in Table 1, the length of spray flame was about 150 mm. Therefore, the substrate was immersed in the flame when the spray distance was kept at 100 mm. Because the deposited anatase will transform to rutile by postheating as revealed by the annealing treatment, it is reasonable to consider the rutile phase presented in the coating

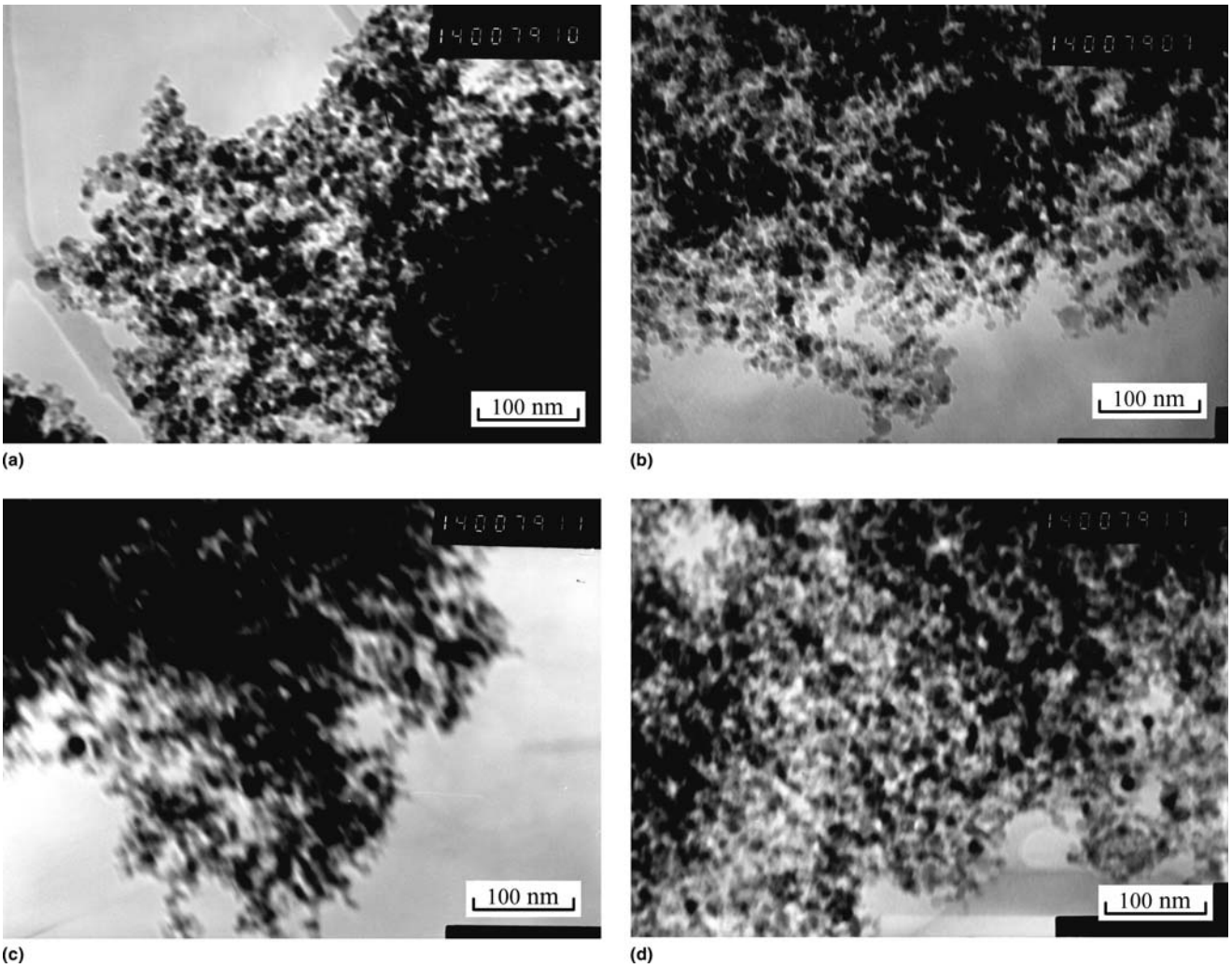

Fig. 6 (a) Morphologies of the nanoparticles within the as-sprayed TiO_2 coating and the coatings annealed at different temperatures: (b) 650 °C, (c) 750 °C, (d) 800 °C

resulted from the phase transformation of the deposited anatase TiO_2 due to the annealing effect of the flame. Moreover, when the deposition was carried out at flame powers of 17 or 21.8 kW, the flame length increased. As a result, the substrate was covered by a more intensive spray flame at higher flame power, and consequently, more anatase phase transformed to rutile phase.

5. Conclusions

The nanostructured TiO_2 coating was flame-sprayed with liquid feedstock at different parameters. The coating containing essentially anatase phase can be deposited at a long spray distance. The heating of the deposited coating by spray flame led to the phase transformation from anatase to rutile, which is responsible for the formation of rutile phase in the coating. The XRD results showed that the significant phase transformation from anatase to rutile by annealing treatment occurred at the temperature higher than 600 °C. It was found that the grain size of rutile was always larger than that of anatase in the as-sprayed coating

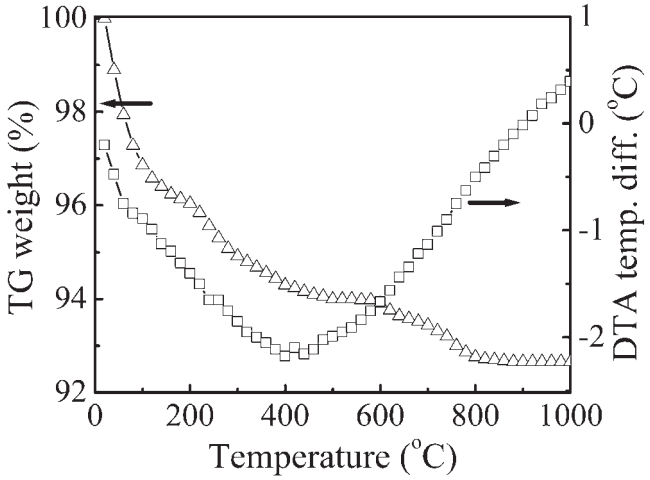

Fig. 7 TG-DTA curves of the as-deposited TiO_2 coating

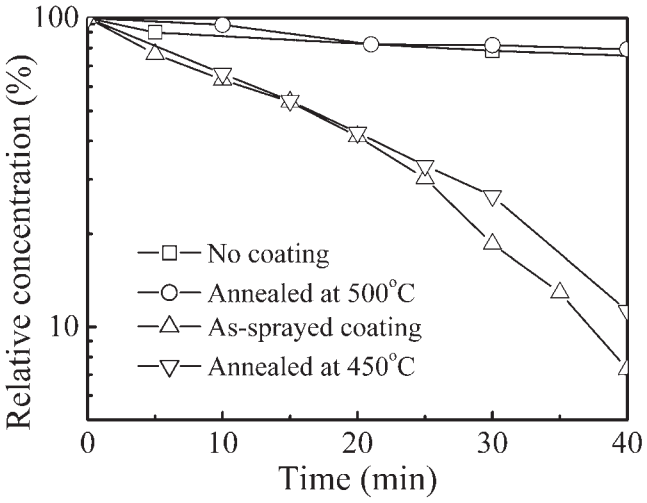

Fig. 8 Change of the relative concentration of acetaldehyde with irradiation time using typical TiO_2 coatings compared with the result obtained without coating

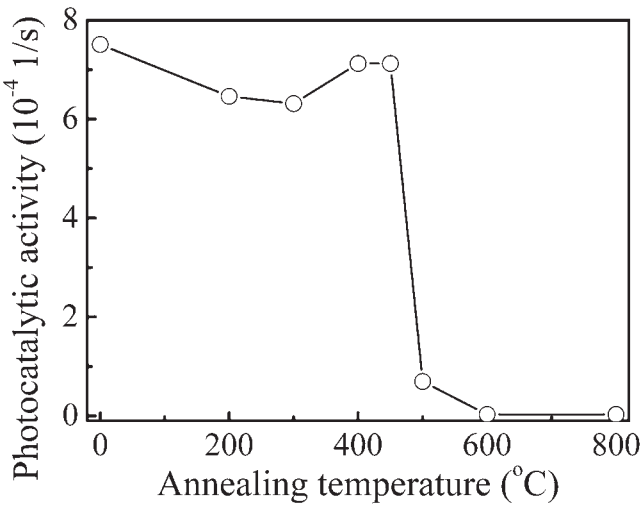

Fig. 9 Effect of annealing temperature on the photocatalytic activity of the TiO_2 deposit

and annealed coatings despite the phase content in the coating. The deposits annealed at temperatures lower than 450 °C were photocatalytically active. However, the deposit annealed at the temperature of 500 °C became photocatalytically inactive, although the coating contained about 95% anatase crystalline. Regarding the initiating phase transformation temperature from anatase to rutile suggested by thermal analyses, it can be proposed that the nucleation of the rutile crystalline starts at the surface of nanoparticles during the phase transformation from anatase to rutile in nanoparticle. The rutile phase grows preferably along the surface. The preferable growth of rutile crystalline near particle surface layer results in the formation of a shell of rutile covering on the anatase core. The phase formation in flame spray deposition of nanostructured TiO_2 with liquid feedstock, the phase transformation during annealing treatment of nanostructured TiO_2, and the change of the photocatalytic performance of the TiO_2 coatings with annealing treatment can be reasonably explained by the present model.

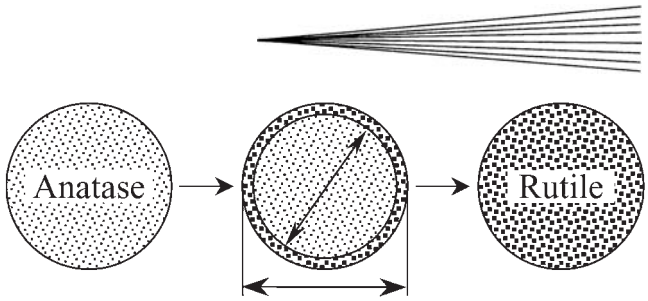

Fig. 10 Schematic diagram for phase transformation of the TiO_2 nanoparticle

Acknowledgments

The present project was supported by the National Natural Science Foundation of China (Grant No. 50071044) and the Education Promotion Project of Xi'an Jiaotong University.

References

1. A. Fujishima and K. Honda, Electrochemical Photolysis of Water at a Semiconductor Electrode, *Nature,* 1972, *238,* p 37-38
2. D.F. Ollis and H. Al-Ekabi, *Photocatalytic Purification and Treatment of Water and Air,* Elsevier, The Netherlands, 1993
3. A. Fujishima, T.N. Rao, and D.A. Tryk, Titanium Dioxide Photocatalysis, *J. Photochem. Photobiol. C,* Vol 1, 2000, p 1-21
4. U. Diebold, The Surface Science of Titanium Dioxide, *Surf. Sci. Rep.,* Vol 48, 2003, p 53-229
5. G-J. Yang, C-J. Li, F. Han, and A. Ohmori, Microstructure and Photocatalytic Performance of High Velocity Oxy-fuel Sprayed TiO_2 Coatings, *Thin Solid Films,* Vol 466 (No. 1-2), 2004, p 81-85
6. H.P. Maruska and A.K. Ghosh, Photocatalytic Decomposition of Water at Semiconductor Electrodes, *Solar Energy,* Vol 20, 1978, p 443-458
7. M. Anpo, T. Shima, S. Kodama, and Y. Kubokawa, Photocatalytic Hydrogenation of CH_3CCH with H_2O on Small-particle TiO_2: Size Quantization Effects and Reaction Intermediates, *J. Phys. Chem.,* Vol 91, 1987, p 4305-4310
8. P. Rivera, K. Tanaka, and T. Hisanaga, Photocatalytic Degradation of Pollutant over TiO_2 in Different Crystal Structures, *Appl. Catal. B,* Vol 3, 1993, p 37-44
9. C-J. Li, G-J. Yang, and Z. Wang, Effect of Spray Parameters on the Structure of Nano-Structured TiO_2 Deposits by Liquid Flame Spray Process, *International Thermal Spray Conference,* E. Lugscheider and C.C. Berndt, Ed., DVS Deutscher Verband für Schweißen, Düsseldorf, Germany, 2002, p 544-549
10. Y-J. Kim and L.F. Francis, Microstructure and Crystal Structure Development in Porous Titania Coatings Prepared from Anhydrous Titanium Ethoxide Solutions, *J. Mater. Sci.,* Vol 33, 1998, p 4423-4433
11. C. Suresh, V. Biju, P. Mukundan, and K.G.K. Warrier, Anatase to Rutile Transformation in Sol-gel Titania by Modification of Precursor, *Polyhedron,* Vol 17, 1998, p 3131-3135
12. B. Xia, H.Z. Huang, and Y.C. Xie, Heat Treatment on TiO_2 Nanoparticles Prepared by Vapor-phase Hydrolysis, *Mater. Sci. Eng. B,* Vol 57, 1999, p 150-154
13. M.P. Zheng, M.Y. Gu, Y.P. Jin, H.H. Wang, P.F. Zu, P. Tao, and J.B. He, Effects of PVP on Structure of TiO_2 Prepared by the Sol-gel Process, *Mater. Sci. Eng. B,* Vol 87, 2001, p 197-201
14. J. Karthikeyan, C.C. Berndt, J. Tikkanen, J.Y. Wang, A.H. King, and H. Herman, Nanomaterial Powders and Deposits Prepared by Flame Spray Processing of Liquid Precursors, *NanoStruct. Mater.,* Vol 8, 1997, p 61-74
15. J. Karthikeyan, C.C. Berndt, J. Tikkanen, S. Reddy, and H. Herman, Plasma Spray Synthesis of Nanomaterial Powders and Deposits, *Mater. Sci. Eng. A,* Vol 238, 1997, p 275-286

16. T. Bhatia, A. Ozturk, L. Xie, E.H. Jordan, B.M. Cetegen, M. Gell, X. Ma, and N.P. Padture, Mechanism of Ceramic Coating Deposition in Solution-Precursor Plasma Spray, *J. Mater. Res.,* Vol 17, 2002, p 2363-2372
17. C-J. Li, G-J. Yang, and Z. Wang, Formation of Nanostructured TiO_2 by Flame Spraying with Liquid Feedstock, *Mater. Lett.,* Vol 57, 2003, p 2130-2134
18. G-J. Yang, C-J. Li, F. Han, and S-F. Mao, Preparation of TiO_2 Photocatalyst by Thermal Spraying with Liquid Feedstock, *Thermal Spray 2003: Advancing the Science and Applying the Technology,* B.R. Marple and C. Moreau, Ed., ASM International, 2003, p 675-680
19. Y. Nosaka, M. Kishimoto, and J. Nishino, Factors Governing the Initial Process of TiO_2 Photocatalysis Studied by Means of In-situ Electron Spin Resonance Measurements, *J. Phys. Chem. B,* Vol 102, 1998, p 10279-10283
20. L. Jing, X. Sun, W. Cai, Z. Xu, Y. Du, and H. Fu, The Preparation and Characterization of Nanoparticle TiO_2/Ti Films and Their Photocatalytic Activity, *J. Phys. Chem. Solids,* Vol 64, 2003, p 615-623